Rotational and Vibrational Relaxation of Methane Excited to $2\nu_3$ in CH_4/H_2 and CH_4/He Mixtures at 296 and 193 K from Double-Resonance Measurements

F. Menard-Bourcin,* C. Boursier, L. Doyennette, and J. Menard

Laboratoire de Physique Moléculaire et Applications, CNRS,
Université Pierre et Marie Curie Boîte 76, 4 place Jussieu, 75252 Paris Cedex 05, France

Received: November 9, 2004; In Final Form: February 9, 2005

A series of time-resolved IR−IR double-resonance experiments have been conducted where methane molecules are excited into a selected rovibrational level of the $2\nu_3(F_2)$ vibrational substate of the tetradecad and where the time evolution of the population of the various energy levels is probed by a tunable continuous wave laser. The rotational relaxation and vibrational energy transfer processes occurring in methane upon inelastic CH_4-H_2 and CH_4−He collisions have been investigated by this technique at room temperature and at 193 K. By probing transitions in which either the lower or the upper level is the laser-excited level, rotational depopulation rates in the $2\nu_3(F_2)$ substate were measured. The rate constants for CH_4-H_2 collisions were found to be 17.7 ± 2.0 and 18.9 ± 2.0 μs^{-1} $Torr^{-1}$ at 296 and 193 K, respectively, and for CH_4−He collisions they are 12.1 ± 1.5 and 16.0 ± 2.0 μs^{-1} $Torr^{-1}$ at the same temperatures. The vibrational relaxation was investigated by probing other stretching transitions such as $2\nu_3(F_2) - \nu_3$, $\nu_3 + 2\nu_4 - 2\nu_4$, and $\nu_3 + \nu_4 - \nu_4$. A kinetic model, taking into account the main collisional processes connecting energy levels up to 6000 cm^{-1}, that has been developed to describe the various relaxation pathways allowed us to calculate the temporal evolution of populations in these levels and to simulate double-resonance signals. The different rate coefficients of the vibrational relaxation processes involved in these mixtures were determined by fitting simulated signals to the observed signals corresponding to assigned transitions. For vibration to translation energy transfer processes, hydrogen is a much more efficient collision partner than helium, nitrogen, or methane itself at 193 K as well as at room temperature.

I. Introduction

In addition to its fundamental interest, the detailed knowledge of vibro-rotational relaxation of methane is essential for understanding and predicting the infrared emission of a wide variety of media in nonlocal thermodynamic equilibrium (non-LTE), in particular in the atmospheres of giant planets. Indeed, methane is present in the atmospheres of planets such as Jupiter and Saturn, and emissions of methane near 3.3 μm, due to non-LTE effects,[1] have been observed in spectra of these planets obtained by the ISO satellite. The modeling of these spectra requires reliable data on vibro-rotational energy transfer processes occurring in methane under the effect of collisions with the main constituents of the atmosphere of these giant planets: hydrogen and helium. Of course, for such applications, the relaxation of CH_4 must be investigated at low temperature.

Similar phenomena are also occurring in the Earth's atmosphere with N_2 and O_2 as collision partners.[2]

Collisional energy transfer in methane has been the subject of numerous experimental and theoretical studies for nearly three decades. Concerning the rotational energy transfer, most results were obtained from spectroscopic measurements involving the various polyads (dyad, pentad, octad, tetradecad, Polyad 6, ...); direct measurements of rotational depopulation rates have been performed at room temperature, in neat methane for octad[3] and for tetradecad[4] levels and in CH_4/N_2 mixtures[5] by using a time-resolved double-resonance (DR) technique. Rotational relaxation rates were measured also at 193 K for CH_4-CH_4 as well as CH_4-N_2 collisions.[6] But no such direct measurements have been performed in CH_4/He nor in CH_4/H_2 mixtures. Concerning the vibrational relaxation, the most extensive study of vibrational energy transfer in methane and in methane mixtures has been made by Moore et al.[7−9] using the laser-excited vibrational fluorescence technique. But these measurements were performed only at room temperature. The only previous low-temperature data were obtained by Perrin and Jolicard[10] by means of photoacoustic measurements and by Siddles et al.[11] by laser-induced infrared fluorescence; they involve the CH_4/He system but not CH_4/H_2.

The present paper is dedicated to the study of the CH_4/H_2 and CH_4/He mixtures at room temperature and at 193 K. This work is a continuation of previous studies[4−6] of the vibro-rotational energy transfer processes implied in the relaxation of CH_4 after its excitation into selected rovibrational levels of the $2\nu_3(F_2)$ vibrational substate by a pulsed laser radiation around 6000 cm^{-1}. In these previous studies, it has been shown that the time-resolved IR−IR DR technique is particularly well-suited to this subject if numerous transitions are found in various vibrational bands. Recently, a better understanding of the mechanisms involved in the relaxation of CH_4 have been achieved for collisions with nitrogen in the 193−296 K temperature range,[6] and a kinetic model has been proposed.

After a brief description of the experimental procedure in section II, the rotational relaxation will be covered in section III. The vibrational relaxation will be treated in section IV; after a presentation of the experimental results, the kinetic model will

* To whom correspondence should be addressed. Fax: 33 (0)1 44 27 70 33. E-mail: menard@ccr.jussieu.fr.

10.1021/jp0448649 CCC: $30.25
Published on Web 03/22/2005

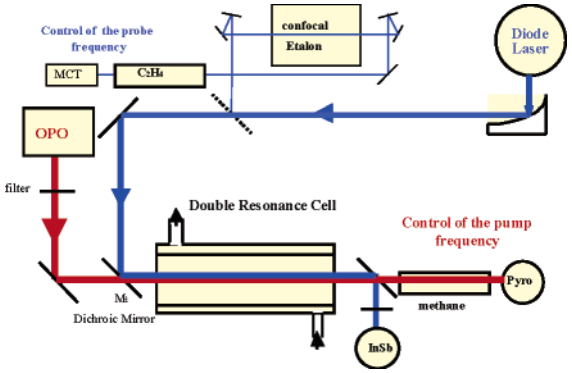

Figure 1. Experimental setup.

be recalled and the results in matters of rate constants for the implied processes will be discussed.

II. Experimental Setup

The DR experimental setup used to investigate the collisional relaxation of methane excited to $2\nu_3(F_2)$ is shown in Figure 1. A detailed description of the experiment can be found in refs 4−6. CH_4 molecules are excited into selected rovibrational levels of the $2\nu_3(F_2)$ vibrational substate near 6000 cm^{-1} by the 7-ns output pulse of an optical parametric oscillator (OPO) pumped by a single-mode pulsed Nd:YAG laser (Continuum); the OPO signal is tunable in the spectral range 1.45−2.12 μm with a line width smaller than 0.02 cm^{-1}. The collision-induced time evolution of populations consecutive to laser excitation is monitored by the low-power beam of a continuous single-mode lead−salt diode laser (Laser Photonics) tunable in the 2939−2986 cm^{-1} range, which permits probing various transitions of ν_3 harmonic and combination bands.

To investigate the relaxation of CH_4 excited into selected rovibrational levels of $2\nu_3(F_2)$, various transitions between polyads have been probed: dyad−octad transitions, $(\nu_3 + \nu_4) \leftarrow \nu_4$ and $(\nu_3 + \nu_2) \leftarrow \nu_2$; pentad−tetradecad transitions, $2\nu_3 \leftarrow \nu_3$ and $(\nu_3 + 2\nu_4) \leftarrow 2\nu_4$; and tetradecad−Polyad 6 transitions, Polyad 6 $\leftarrow 2\nu_3$. A simplified diagram of the CH_4 vibrational levels with the main probed transitions is given in Figure 2.

The pumping and probing beams propagate collinearly through the DR cell that is a variable temperature cell allowing operation at low temperatures down to 190 K. It is a triple-walled Pyrex tube, 68 cm in length and 3.8 cm in internal diameter. The outer vacuum jacket is for thermal insulation, and the intermediate one is for cooling the sample cell by flowing cold ethanol from a refrigerator (Maton) at a regulated temperature. The cell temperature is monitored by a chromel−alumel thermocouple placed in the cooling jacket. During the experiments, the temperature fluctuations did not exceed ±0.5 K.

Our measurements have been performed in CH_4/H_2 and CH_4/He mixtures at 296 and 193 K for different gas pressures from 0.01 to 40 Torr and by varying the methane molar fraction in the gas mixtures from 1 to 100%.

III. Rotational Relaxation

A. Experimental Results. As is well-known, the fastest process occurring after excitation of methane in a well-defined level of the $2\nu_3(F_2)$ substate is rotational relaxation. The laser-excited rotational level is rapidly depleted as the energy is redistributed among the other rotational levels of the same spin modification (same rovibrational symmetry type A, E, or F) in the $2\nu_3$ state. This is because collisions are very inefficient in changing the nuclear spin. The depopulation of a selected rotational level is directly observed by probing a Polyad 6−$2\nu_3$-(F_2) transition in which the lower level is the one excited by the laser pulse. Two such typical DR signals obtained in pure methane and in a CH_4/He mixture with the same total gas pressure at 193 K are shown in Figure 3.

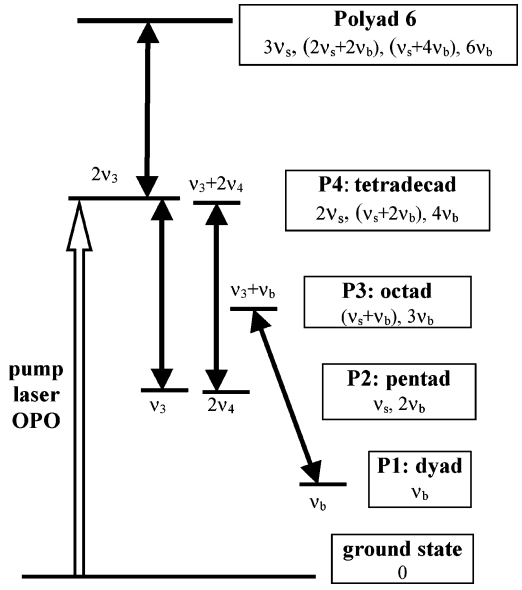

Figure 2. Simplified diagram of the vibrational energy levels up to 6000 cm^{-1} showing the main transitions probed in this work. "b" is for bending, and "s" is for stretching; $\nu_b = \nu_2$ or ν_4 and $\nu_s = \nu_1$ or ν_3.

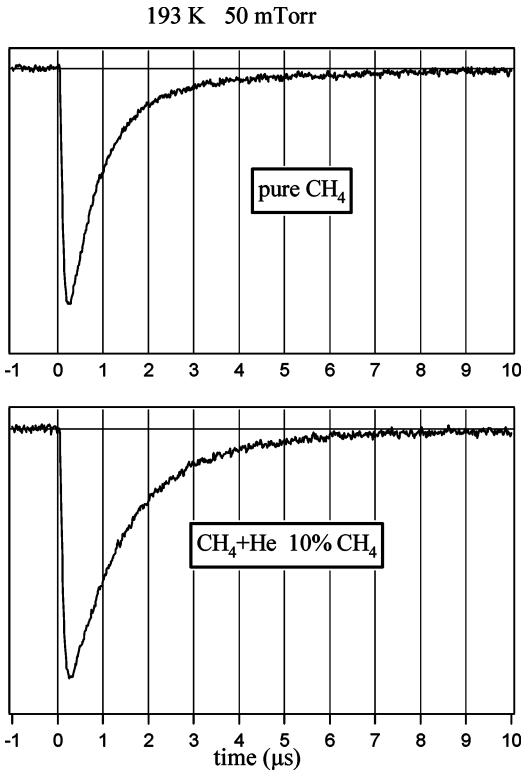

Figure 3. DR signals showing the rotational depopulation of the $J = 3$ level by self-collision and CH_4−He collisions. They were obtained by exciting methane into the $2\nu_3(F_2)$, $J = 3$, A_1, 32 level via the Q_3 line of the $2\nu_3(F_2)-0$ band at 6004.29 cm^{-1} and by tuning the laser diode to 2944.82 cm^{-1}, which corresponds to a Polyad 6−$2\nu_3(F_2)$ transition, the lower level of which is the laser-excited level.

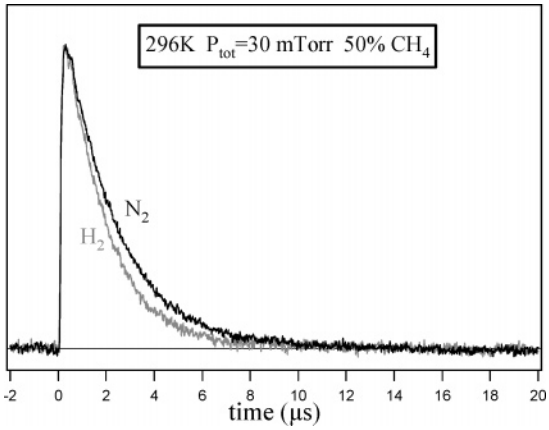

Figure 4. DR signals obtained at room temperature by exciting CH_4 molecules into the $2\nu_3(F_2)$, $J = 1$, A_2, 18 level and by probing the consecutive evolution of the excited state with the laser diode tuned to the transition $2\nu_3(F_2)$, $J = 1$, A_2, 18 ← ν_3, $J = 2$, A_1, 4 at 2963.99 cm^{-1}. The depopulation of the excited level is slower in nitrogen than in hydrogen.

These time-resolved signals were obtained, at 193 K, by exciting methane into the $2\nu_3(F_2)$, $J = 3$, A_1, 32 level[12] and by tuning the laser diode frequency to a Polyad $6-2\nu_3(F_2)$ transition, the lower level of which is the laser-excited level. These signals exhibit first a quasi-instantaneous decay in transmission of the probe beam (in the limit of electronic response), due to the increase in population of the laser-excited rotational level, followed by a rise due to the depletion of this level by collisional processes of rotational energy transfer. The signal obtained in neat methane exhibits a faster rise than that obtained in the CH_4/He mixture with a methane molar fraction $z = 0.1$. This shows that CH_4-He collisions are less efficient for rotational relaxation of CH_4 than self-collisions. Such DR signals may be analyzed by fitting the rising part of the curve to a sum of two exponential functions of time. The pressure-dependent rotational relaxation rate is extracted from the fastest exponential that is also the strongest one. In mixtures involving identical methane partial pressure, the rate varies linearly with the foreign gas pressure and the rate constant of rotational relaxation corresponding to CH_4-foreign gas collisions is deduced from the slope of this linear variation.

Another type of probe transition has been used to investigate the rotational relaxation: the probe laser is tuned to a $2\nu_3(F_2)-\nu_3$ transition, the upper level of which is the rotational level excited by the pump laser. In this case, the DR signals exhibit an initial amplification followed by a fast decay with a temporal variation opposite to that observed before.

At 296 K, hydrogen is a collision partner more effective than nitrogen[5] and it is almost as effective as methane itself for the rotational relaxation. An example is given in Figure 4: the DR signals presented were obtained by exciting CH_4 molecules, via the R_0 line of the $2\nu_3$ band, into the level $2\nu_3(F_2)$, $J = 1$, A_2, 18 and by probing the consecutive evolution of the excited state with the laser diode tuned to the $2\nu_3(F_2)$, $J = 1$, A_2, 18 ← ν_3, $J = 2$, A_1, 4 transition at 2963.99 cm^{-1}. At 193 K, hydrogen is a collision partner similar to nitrogen for the rotational relaxation of methane: the depopulation of the excited level is about as fast in nitrogen as in hydrogen. At room temperature as well as at 193 K the rotational relaxation is slower by collisions with helium than by collisions with hydrogen or nitrogen.

Various pump−probe combinations have been found allowing us to determine the relaxation rates of the $J = 1$ to $J = 4$ levels of $2\nu_3(F_2)$. The main probe wavenumbers used in this work are given in Tables 1 and 2. After a series of measurements performed in various mixture and pressure conditions by probing either the Polyad $6-2\nu_3(F_2)$ or $2\nu_3(F_2)-\nu_3$ transitions, the rotational relaxation rate constant, that is, the rotational relaxation rate divided by the total pressure, was found to vary linearly with the molar fraction *z*. A linear regression has yielded the following values for the rotational relaxation rate constants: 17.7 ± 2.0 and 18.9 ± 2.0 μs^{-1} $Torr^{-1}$ for CH_4-H_2 collisions at 296 and 193 K, respectively, and 12.1 ± 1.5 and 16.0 ± 2.0 μs^{-1} $Torr^{-1}$ for CH_4-He collisions at the same temperatures. No significant difference was observed between the rotational rate constants of the $2\nu_3(F_2)$ rotational levels investigated in the present study, namely, *A* symmetry levels with *J* ranging from 1 to 4. Let us recall that the corresponding values that we have previously obtained for CH_4-CH_4 collisions[4,6] are 20.8 ± 2.5 and 28.3 ± 3.0 μs^{-1} $Torr^{-1}$. All these results are gathered in Table 3 along with those previously obtained in CH_4/N_2 mixtures.[5,6]

TABLE 1: Main Frequencies Used To Probe Transitions Polyad 6 ← $2\nu_3(F_2)$

probe frequency (cm^{-1})	$2\nu_3(F_2)$ level *JCN*	pump line populating this level	$2\nu_3(F_2)$ level energy	Polyad 6 level energy
2959.66	$J = 1$, A_2, 18	R(0)	6015.66	8975.32
2964.16	$J = 4$, A_2, 43	Q(4)	6108.67	9072.83
2944.53	$J = 2$ A_1, 29	P(3)	6035.01	8979.54
2944.82	$J = 3$, A_1, 32	Q(3)	6067.17	9011.99
2939.79	$J = 4$, A_2, 43	Q(4)	6108.67	9048.46

TABLE 2: Main Frequencies Used To Probe Transitions $2\nu_3(F_2)$ ← ν_3 with Their Assignments

probe frequency (cm^{-1})	$2\nu_3(F_2)$ level *JCN*	$2\nu_3(F_2)$ level energy	ν_3 level *JCN*	ν_3 level energy
2944.69	$J = 3$, A_1, 32	6067.17	$J = 4$, A_2, 5	3122.48
2945.07	$J = 3$, A_2, 40	6065.64	$J = 4$, A_1, 7	3120.57
2951.23	$J = 2$, A_1, 29	6035.01	$J = 3$, A_2, 6	3083.78
2963.99	$J = 1$, A_2, 18	6015.66	$J = 2$, A_1, 4	3051.67
2983.39	$J = 3$, A_1, 32	6067.17	$J = 3$, A_2, 6	3083.78
2985.95	$J = 6$, A_2, 65	6222.44	$J = 6$, A_1, 9	3236.49
2985.09	$J = 6$, A_1, 71	6222.51	$J = 6$, A_2, 8	3237.41

B. Discussion. For lack of other available time-resolved relaxation measurements, our results can only be compared to pressure broadening data. Numerous measurements of H_2-broadened widths have been performed at room temperature in different vibrational bands. They range from 0.055 to 0.075 cm^{-1} atm^{-1} with a mean value of 0.065 cm^{-1} atm^{-1} for the ν_3 and ν_4 bands[13−15] and from 0.066 to 0.075 cm^{-1} atm^{-1} for the $2\nu_3$ and $3\nu_3$ bands.[16,17] Assuming that the upper and lower levels of a given transition have the same total depopulation rate constant *k*, the pressure broadening coefficient γ/P may be approximately related to *k* by the following formula: $\gamma/P = k/2\pi c$ where *c* is the velocity of light in vacuum. Using this formula, we can deduce from our results a value of 0.071 ± 0.008 cm^{-1} atm^{-1} for the equivalent broadening coefficient upon CH_4-H_2 collisions at room temperature. This value is close to the values measured by infrared spectroscopy for the $2\nu_3$ band. At low temperature, our results lead, using the same formula, to a broadening coefficient of 0.076 ± 0.008 cm^{-1} atm^{-1}. This can be compared to results obtained for ν_4 at 200 K by Margolis,[14] 0.076−0.081 cm^{-1} atm^{-1}, or at 209 K by Varanasi and Chudamani,[15] 0.055−0.076 cm^{-1} atm^{-1}.

Measurements of He-broadened line widths at room temperature yield results from 0.042 to 0.048 with a mean value of 0.046 cm^{-1} atm^{-1} for the $2\nu_3$ band[16,18] which is close to the equivalent broadening coefficient deduced from our rate constant

TABLE 3: Values of the Rotational Relaxation Rate Constants of Methane Determined at 193 K and at Room Temperature for the Collision Partners Studied in This Work (H_2 and He) or Previously (CH_4 and N_2; Refs 4−6)

	193 K		296 K	
collision partner	s^{-1} $Torr^{-1}$	s^{-1} cm^3 $molecule^{-1}$	s^{-1} $Torr^{-1}$	s^{-1} cm^3 $molecule^{-1}$
He	$(16.0 \pm 2.0) \times 10^6$	$(3.20 \pm 0.40) \times 10^{-10}$	$(12.1 \pm 1.5) \times 10^6$	$(3.71 \pm 0.46) \times 10^{-10}$
H_2	$(18.9 \pm 2.0) \times 10^6$	$(3.78 \pm 0.40) \times 10^{-10}$	$(17.7 \pm 2.0) \times 10^6$	$(5.43 \pm 0.61) \times 10^{-10}$
N_2	$(21.5 \pm 3.0) \times 10^6$	$(4.30 \pm 0.6) \times 10^{-10}$	$(13.0 \pm 1.5) \times 10^6$	$(3.99 \pm 0.46) \times 10^{-10}$
CH_4	$(28.3 \pm 3.0) \times 10^6$	$(5.66 \pm 0.60) \times 10^{-10}$	$(20.8 \pm 2.5) \times 10^6$	$(6.38 \pm 0.77) \times 10^{-10}$

measurements: 0.049 ± 0.006 cm^{-1} atm^{-1}. The value found here at 193 K, 0.065 ± 0.008 cm^{-1} atm^{-1}, is higher than the values found for the $2\nu_3$ band[19] but in better agreement with the values found[20] for the ν_3 band, 0.056 ± 0.005 cm^{-1} atm^{-1} at 190 K.

IV. Vibrational Relaxation

As previously seen, after laser excitation of CH_4 molecules on a single rovibrational level of given symmetry type A, E, or F, the fast rotational relaxation is redistributing the energy on all the rotational levels of the same symmetry type within the $2\nu_3(F_2)$ substate. Once this transient equilibrium is reached, energy and, hence, population are redistributed over the other vibrational states.

A. Experimental Results. The vibrational relaxation was investigated by monitoring the time evolution of the population of several vibrational states from the dyad to the tetradecad using well-identified DR signals corresponding to stretching transitions $\Delta v_3 = \pm 1$. Although data available in the literature on the methane molecule spectroscopy are rather incomplete, in particular for states above the pentad, we have been able to find a lot of interesting transitions by scanning the frequency of the probe laser. By using all the types of probe at our disposal we have been able to visualize the temporal evolution of populations in various vibrational energy states implied in the relaxation of CH_4 molecules.

1. Tetradecad States and Pentad States. The depopulation of the $2\nu_3$ vibrational state is well-observed when the probe laser is tuned to a transition between a $2\nu_3$ level of the tetradecad not directly pumped by the laser and a state of the sixth polyad (located higher in energy and, hence, not populated in the relaxation process). A number of pump−probe combinations have been used. The signals shown in Figure 5 have been obtained by probing this type of transition; the lower level of the probed transition is the $J = 3$ level while the rotational level directly excited by laser is the $J = 1$ level. Pressures are one order of magnitude larger than in the previous examples; it can be seen that the vibrational energy transfer processes that spread out energy from the $2\nu_3(F_2)$ state to other vibrational states are slower than the rotational relaxation by about one order of magnitude. After laser excitation, the decrease in transmission of the probe beam corresponds to the filling of the lower level of the probed transition, that is, $2\nu_3(F_2)$, $J = 3$, A_1, 32, by rotational energy transfer from the laser-excited level $2\nu_3(F_2)$, $J = 1$, A_2, 18. The following increase in transmission corresponds to depopulation of the $2\nu_3(F_2)$ vibrational substate. This depopulation is clearly slower in CH_4/H_2 mixtures than in pure methane. At 193 K, it is also slower than in CH_4/He mixtures. At room temperature, no significant differences were observed between the CH_4/He and the CH_4/H_2 mixtures. For CH_4/He mixtures, the depopulation of the $2\nu_3(F_2)$ substate shows a weak dependence with temperature: it is slightly slower at room temperature than at 193 K for a given pressure and it is faster for a given total number density. For CH_4/H_2 mixtures, the depopulation of the $2\nu_3(F_2)$ state is faster at room temperature than at 193 K for a given pressure as for a given total number density.

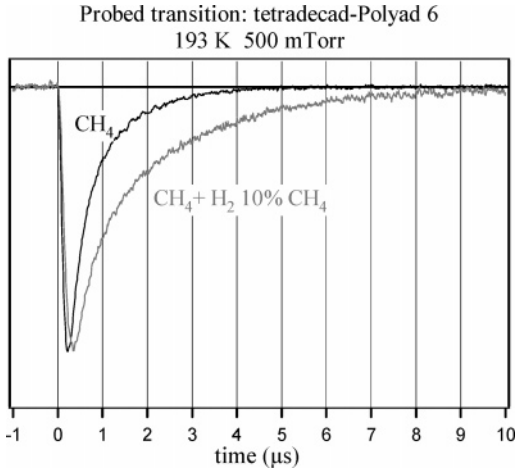

Figure 5. DR signals showing the vibrational depopulation of the $2\nu_3$ state by self-collisions and by CH_4-H_2 collisions. The total pressure is 10 times higher than in Figure 3. The tetradecad−Polyad 6 probed transition is at 2944.82 cm^{-1}.

When the probe laser is tuned to a transition between the pentad and the tetradecad, the depopulation of the tetradecad is observed as well as the filling of the pentad states. For instance, by probing a $2\nu_3(F_2)-\nu_3$ transition, a large increase in transmission of the probe beam is observed after the laser excitation. It corresponds to the filling of the upper level of the probed transition by rotational energy transfer. Then, the transmitted intensity decreases upon the combined effect of the depopulation of the $2\nu_3(F_2)$ state and of the filling of the ν_3 lower level which leads to a transient absorption of the probe beam. The temporal evolution of this type of signal is very similar to what was observed previously in CH_4/N_2 mixtures.[6]

For other transitions between the tetradecad and the pentad, we have observed many interesting signals but the wavenumbers do not correspond to any assigned or predicted transition except for one line that is assigned to a transition between a $2\nu_4$ level of the pentad and a $(2\nu_4 + \nu_3)$ level of the tetradecad according to the calculations provided by Robert and Champion[21] using the spherical top data system software.[22]

When the probe laser is tuned to a transition between a $2\nu_4$ level of the pentad and a $(2\nu_4 + \nu_3)$ level of the tetradecad, the amplified part of the IR DR signals is weaker and the absorbed one is larger than by probing a $2\nu_3(F_2)-\nu_3$ transition. The $2\nu_4$ state is the lower state of the pentad, and when the pentad states are equilibrated the maximum of the population is in this state. The temporal evolution of this type of signal in CH_4/He mixtures is very similar to what was previously observed in CH_4/N_2 mixtures,[6] but it is significantly different in CH_4/H_2 mixtures as shown in Figure 6.

The population of the $2\nu_4$ state evolves clearly faster by collision with hydrogen than by collisions with helium. The pentad states are populated and depleted both by cascading V−V transfer processes that occur through the exchange of one

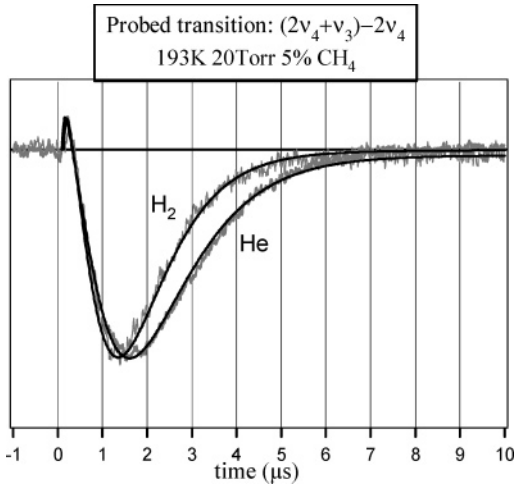

Figure 6. DR signals attributed to a $(2\nu_4 + \nu_3) - 2\nu_4$ transition in CH_4/H_2 and CH_4/He mixtures with 5% CH_4 at 20 Torr pressure and 193 K. Simulated signals (full line) are superimposed.

vibrational quantum between two methane molecules and by vibration to translation and rotation (V−T) energy transfer processes occurring upon collisions with the foreign gas. Actually, for such a molar fraction, while the V−V transfer processes still play a leading part in the depletion of the pentad states and in the filling of dyad states for CH_4/N_2 and CH_4/He mixtures, this is no longer true for CH_4/H_2 mixtures.

Concerning the temperature dependence, all the signals obtained by probing transitions between pentad and tetradecad levels are faster at 193 K than at room temperature for the same mixture at the same pressure.

2. Dyad States. The evolution of populations in the dyad is monitored by probing dyad−octad transitions. A similar temporal behavior of the DR signals is observed for $(\nu_4 + \nu_3) - \nu_4$ and $(\nu_2 + \nu_3) - \nu_2$ transitions, but the DR signals depend on the symmetry type (A, E, or F) of the probed transition relative to the symmetry or spin modification of the methane molecules excited by the pumping pulse.

For instance, when the methane molecules are excited onto an A-symmetry-type level, the increase in population of the A symmetry levels is faster than for the other symmetry levels as shown in Figure 7. The transient excess in populations of the A-symmetry levels of the dyad compared to the levels of symmetry E and F is due to the conservation of the spin modification in collisional processes. Indeed, the dyad states are populated both by V−T transfer processes and by V−V transfer processes.

In a cascading V−T de-excitation scheme starting from an A-symmetry excited level, only A-symmetry levels should be populated while in near resonant V−V transfer processes involving the exchange of a ν_4 vibrational quantum between two methane molecules, one molecule excited in a tetradecad A-symmetry level gives one molecule in an A-symmetry level of the octad by loss of a bending quantum while another molecule is promoted from the ground state to the dyad, keeping its spin modification (either A, E, or F) and so on from the octad to the pentad and from the pentad to the dyad. Consequently, the filling of the F-symmetry levels is due to the promotion of molecules from the ground state whereas the filling of the A-symmetry levels is due both to the promotion from the ground state and to the de-excitation from the upper levels. It should be noted that some molecules of F-symmetry type are excited to the pentad by ν_3 exchange, but we have observed that this process is significantly slower than ν_4 exchange. This

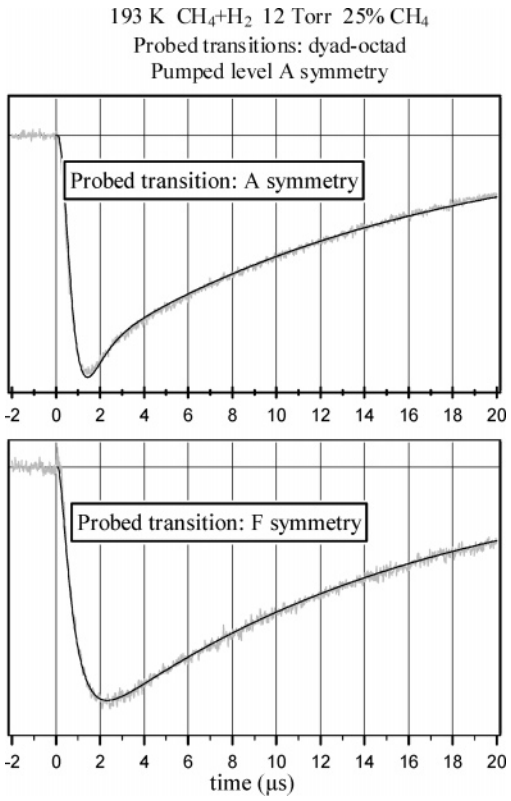

Figure 7. DR signals for a CH_4/H_2 mixture (in grey) showing the redistribution of molecules over the different symmetry species. Simulated signals (in black) are in fair agreement with the experimental ones. DR signals are obtained at 193 K with 25% CH_4 at 12 Torr total pressure. Methane molecules are excited to an A-symmetry-type level via the R_0 line.

implies a temporary excess in the population of the A-symmetry levels in the dyad with respect to the equilibrium distribution of the different spin modifications (5/16 in A, 2/16 in E, and 9/16 in F). This temporary excess disappears by ν_4 exchange between the dyad and the ground state which is called vibrational swap. Vibrational exchange occurs between methane molecules until an equilibrium is obtained in the distribution of the molecules in the various spin modifications. Then all the dyad levels return to Boltzmann equilibrium by V−T transfer processes and, for all dyad−octad probes, the decrease in absorption of the corresponding DR signals proceeds at the same rate.

Helium is more efficient than nitrogen[5,6] but less efficient than methane as a collision partner for the de-excitation of the dyad. Hydrogen is a much more efficient collision partner than helium as can be seen in Figure 8 obtained by exciting methane into an A-symmetry level via the R_0 transition. The signals obtained for the CH_4/He mixture are clearly slower than for the CH_4/H_2 mixture.

Actually, hydrogen is also a much more efficient partner in the vibrational thermalization of methane than nitrogen and methane itself. The rate of V−T transfer processes (loss of a bending quantum) is two orders of magnitude higher in hydrogen than in nitrogen. For this reason, whereas in CH_4/N_2 mixtures[6] V−V transfer processes (exchange of a vibrational quantum between two molecules of methane) play a major role in the relaxation of methane down to 1% methane molar fraction, it is no more the case in CH_4/H_2 mixtures.

When the temperature decreases from room temperature to 193 K, V−T transfer processes become slower while vibration−vibration transfer processes are faster in respect to pressure and

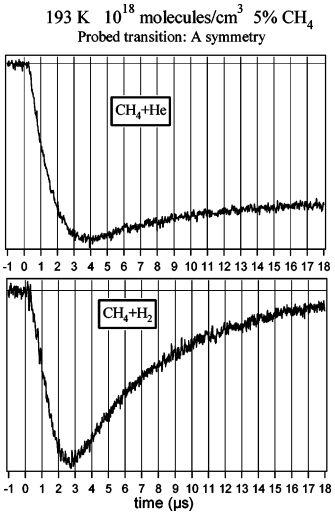

Figure 8. DR signals obtained by probing a dyad−octad transition at 193 K in a CH_4/He and a CH_4/H_2 mixture with 5% CH_4 at 20 Torr total pressure. Methane molecules are excited to an A-symmetry-type level via the R_0 line.

also in respect to total number density. The V−T transfer processes have a positive dependence on temperature, and the V−V processes have a negative one which results in a faster filling and a slower depletion of the dyad levels at low temperature.

B. Kinetic Model. To derive from the observed DR signals the rate constants of the various processes, it is necessary to build a numerical kinetic model, taking into account the large number of relevant collisional processes connecting energy levels up to 6000 cm^{-1}. Such a model has been developed to describe the vibrational relaxation of methane in neat gas and in CH_4/N_2 mixtures.[6] This model has allowed us to reproduce rather precisely the experimental DR signals at room temperature as well as at 193 K and to obtain rate coefficients of energy transfer processes. We briefly recall here the main features of the selected model.[6] Considering the complexity of the energy levels of methane and because the molecules are excited rather high in energy (6000 cm^{-1}), only the vibrational aspect of the relaxation is taken into account. As described in section II, the average rotational de-excitation rate is fast enough, even for CH_4−He collisions, to ensure rotational equilibration in each state considered in the model for the time × pressure scales used to study vibrational relaxation. The system considered in the kinetic model involves 90 states from the ground state to the tetradecad: 30 vibrational energy states and for each of them we take into account the overall rovibrational symmetry S = A, E, or F (related to the total nuclear spin). We introduce below the various processes coupling the vibrational states involved in the model.

(1) Energy Transfer Processes. There are three main types of energy transfer processes involved in vibrational relaxation through molecular collisions.

Intermode Energy Transfer Processes. Intermode transfers spread out the vibrational energy within a polyad, leading to a distribution of energy among the interacting states of the polyad. These processes conserve the symmetry and can occur upon self-collisions as well as CH_4−M collisions. The processes considered here are (i) transfer between stretching modes $\nu_3 \leftrightarrow \nu_1$ such as

$$CH_4(\nu_3, S) + M \leftrightarrow CH_4(\nu_1, S) + M \quad (1)$$

for the pentad and similar processes in the other polyads; (ii) transfer between bending modes $\nu_2 \leftrightarrow \nu_4$ such as

$$CH_4(\nu_2, S) + M \leftrightarrow CH_4(\nu_4, S) + M \quad (2)$$

for the dyad and similar processes in the other polyads; and (iii) transfer between stretching and bending modes. We limited ourselves to transfer between the ν_3 and $(\nu_2 + \nu_4)$ modes which are known as strongly interacting such as

$$CH_4(\nu_3, S) + M \leftrightarrow CH_4(\nu_2 + \nu_4, S) + M \quad (3)$$

for the pentad and similar processes in the other polyads.

Near-Resonant Vibration−Vibration Energy Transfer Processes. Near-resonant vibration−vibration (V−V) energy transfer processes involve the exchange of one vibrational quantum between two CH_4 molecules and occur only upon self-collisions. These processes distribute the energy among the different polyads: (i) processes involving the exchange of one ν_3 quantum such as

$$CH_4(\nu_3,S) + CH_4(0, AEF) \leftrightarrow CH_4(0, S) + CH_4(\nu_3, AEF) \quad (4)$$

and similar processes linking other polyads and (ii) processes involving the exchange of one ν_4 quantum such as

$$CH_4(\nu_4, S) + CH_4(0, AEF) \leftrightarrow CH_4(0, S) + CH_4(\nu_4, AEF) \quad (5)$$

and similar processes linking other polyads.

They allow also the distribution of vibrational excitation among the different symmetry species. Indeed, because collisions are preserving the total nuclear spin, the return to equilibrium for the different symmetry species is ensured by V−V processes which are called "vibrational swap" such as, for example,

$$CH_4(\nu_4, A) + CH_4(0, F) \leftrightarrow CH_4(0, A) + CH_4(\nu_4, F)$$

V−T Energy Transfer Processes. The vibration to translation, rotation (V−T) energy transfer processes are responsible for the (slow) de-excitation of the gas. The V−T processes considered involve the loss of one ν_4 or ν_2 bending quantum. They can occur upon self-collisions as well as CH_4−M collisions:

$$CH_4(\nu_4, S) + M \leftrightarrow CH_4(0, S) + M \quad (6)$$

$$CH_4(\nu_2, S) + M \leftrightarrow CH_4(0, S) + M \quad (7)$$

and similar processes for the higher polyads.

To limit the number of rate coefficients in the model, some additional assumptions have been made.

(2) Simplifying Assumptions. (a) All $\nu_3 \rightarrow \nu_1$ intermode transfer processes considered in the exothermic direction ($\nu_3 \rightarrow \nu_1$) have the same rate coefficients, $k^{CH_4}_{\nu_3\rightarrow\nu_1}$ for self-collisions and $k^{H_2}_{\nu_3\rightarrow\nu_1}$ or $k^{He}_{\nu_3\rightarrow\nu_1}$ for CH_4-H_2 or CH_4−He collisions. These rate coefficients are those of the direct exothermic process (1).

Similarly, for $\nu_2 \rightarrow \nu_4$ and $\nu_3 \rightarrow \nu_2 + \nu_4$ intermode transfer processes, the rate coefficients $k^{M}_{\nu_2\rightarrow\nu_4}$ and $k^{M}_{\nu_3\rightarrow\nu_2+\nu_4}$ are those of the direct exothermic processes (2) and (3).

(b) The rate coefficients of near-resonant V−V transfer processes are related by a scaling factor appropriate to first-

TABLE 4: Vibrational Energy Transfer Processes and Their Corresponding Rate Coefficients

	193 K		296 K	
processes	s^{-1} Torr^{-1}	cm^3 s^{-1} molecule^{-1}	s^{-1} Torr^{-1}	cm^3 s^{-1} molecule^{-1}
$k^{CH_4}_{\nu_3\rightarrow\nu_1}$	$(1.3 \pm 0.4) \times 10^6$	$(2.6 \pm 0.8) \times 10^{-11}$	$(1.1 \pm 0.3) \times 10^6$	$(3.37 \pm 0.92) \times 10^{-11}$
$k^{He}_{\nu_3\rightarrow\nu_1}$	$(0.9 \pm 0.25) \times 10^6$	$(1.8 \pm 0.5) \times 10^{-11}$	$(0.8 \pm 0.3) \times 10^6$	$(2.45 \pm 0.92) \times 10^{-11}$
$k^{H_2}_{\nu_3\rightarrow\nu_1}$	$(0.9 \pm 0.25) \times 10^6$	$(1.8 \pm 0.5) \times 10^{-11}$	$(0.8 \pm 0.3) \times 10^6$	$(2.45 \pm 0.92) \times 10^{-11}$
$k^{CH_4}_{\nu_2\rightarrow\nu_4}$	$(2.4 \pm 0.4) \times 10^6$	$(4.8 \pm 0.8) \times 10^{-11}$	$(2.2 \pm 0.5) \times 10^6$	$(6.75 \pm 1.53) \times 10^{-11}$
$k^{He}_{\nu_2\rightarrow\nu_4}$	$>1.4 \times 10^6$	$>2.8 \times 10^{-11}$	$>1.2 \times 10^6$	$>3.68 \times 10^{-11}$
$k^{H_2}_{\nu_2\rightarrow\nu_4}$	$>1.4 \times 10^6$	$>2.8 \times 10^{-11}$	$>1.2 \times 10^6$	$>3.68 \times 10^{-11}$
$k^{CH_4}_{\nu_3\rightarrow\nu_2+\nu_4}$	$(1.8 \pm 0.2) \times 10^6$	$(3.6 \pm 0.4) \times 10^{-11}$	$(1.5 \pm 0.2) \times 10^6$	$(4.6 \pm 0.6) \times 10^{-11}$
$k^{He}_{\nu_3\rightarrow\nu_2+\nu_4}$	$(1.4 \pm 0.2) \times 10^6$	$(2.8 \pm 0.4) \times 10^{-11}$	$(1.15 \pm 0.15) \times 10^6$	$(3.53 \pm 0.46) \times 10^{-11}$
$k^{H_2}_{\nu_3\rightarrow\nu_2+\nu_4}$	$(0.8 \pm 0.2) \times 10^6$	$(1.6 \pm 0.4) \times 10^{-11}$	$(1.15 \pm 0.15) \times 10^6$	$(3.53 \pm 0.46) \times 10^{-11}$
k_{ν_3}	$(1.4 \pm 0.4) \times 10^5$	$(0.28 \pm 0.08) \times 10^{-11}$	$(8.0 \pm 3.0) \times 10^4$	$(2.45 \pm 0.92) \times 10^{-12}$
k_{ν_4}	$(5.8 \pm 0.3) \times 10^5$	$(1.16 \pm 0.06) \times 10^{-11}$	$(3.6 \pm 0.2) \times 10^5$	$(1.10 \pm 0.04) \times 10^{-11}$
$k^{CH_4}_{V-T}$	$(6.0 \pm 2.0) \times 10^2$	$(1.2 \pm 0.4) \times 10^{-14}$	$(1.05 \pm 0.15) \times 10^3$	$(3.2 \pm 0.5) \times 10^{-14}$
k^{He}_{V-T}	$(2.7 \pm 0.3) \times 10^2$	$(0.54 \pm 0.06) \times 10^{-14}$	$(5.5 \pm 0.5) \times 10^2$	$(1.69 \pm 0.15) \times 10^{-14}$
$k^{H_2}_{V-T}$	$(7.2 \pm 0.3) \times 10^3$	$(1.44 \pm 0.06) \times 10^{-13}$	$(1.20 \pm 0.15) \times 10^4$	$(3.68 \pm 0.5) \times 10^{-13}$

order perturbation theory for harmonic oscillators. For instance, the rate coefficient for the process

$$CH_4(2\nu_3) + CH_4(0) \leftrightarrow CH_4(\nu_3) + CH_4(\nu_3)$$

is twice the rate coefficient of process (4), and the rate coefficient of the process

$$CH_4(4\nu_4) + CH_4(0) \leftrightarrow CH_4(3\nu_4) + CH_4(\nu_4)$$

is four times the rate coefficient of process (5). Hence, only two rate coefficients are necessary. The elementary rate coefficients of processes (4) and (5) are noted k_{ν_3} and k_{ν_4} for the exchange of a ν_3 or a ν_4 quantum, respectively.

(c) The rate coefficients of V−T transfer processes are assumed equal for processes (6) and (7) (ν_2 and ν_4 de-excitation), and for the higher states they are related to each other according to the harmonic oscillator approximation. For instance the rate coefficient of the process

$$CH_4(3\nu_4, S) + M \leftrightarrow CH_4(2\nu_4, S) + M$$

is three times that of process (6). The elementary rate coefficients, that is, those of process (6), are noted k^M_{V-T} for CH_4−M collisions.

All the rate coefficients for the reverse processes are deduced from the direct ones by applying detailed balance.

C. Results and Discussion. From the kinetic model, one obtains a system of coupled nonlinear differential equations which are solved by a Runge−Kutta method. Thanks to this model, one can calculate the time evolution of populations of the different states and generate simulated DR signals directly comparable with the experimental signals. The rate coefficients of the processes introduced into the model are adjusted to obtain the best agreement with the experiments, and the final results are given in Table 4.

At room temperature, the only significant difference between CH_4/N_2, CH_4/H_2, and CH_4/He mixtures is obtained for the rate coefficient of V−T energy transfer. Indeed, as described in section IV.A, the main changes with respect to the collision partner are observed for $(2\nu_4 + \nu_3) - 2\nu_4$ and dyad−octad probes, and the simulated DR signals for these types of probe are mainly dependent on the rate coefficient of the V−T energy transfer and also on the rate coefficient of the V−V energy transfer that is not related to the foreign gas and was previously determined.[4−6] So, the values of the rate coefficients for the intermode transfer processes upon CH_4−He or CH_4-H_2 collisions were kept identical to those obtained for N_2 at room temperature.

The previous observations done at room temperature are still relevant at 193 K for helium. For hydrogen, the value of the rate coefficient at low temperature for the stretching to bending intermode transfer process must be reduced compared to the value obtained for N_2 to take into account the slower depletion of the $2\nu_3(F_2)$ state observed in the DR signals.

Using the rate coefficients of Table 4, the behavior of the signals obtained with dyad−octad probes and particularly the effect of the symmetry of the probed transition with respect to the symmetry of the pumped transition are fairly well-reproduced. Indeed, the simulated signals for two dyad−octad probes of different symmetries shown in Figure 7 are in very good agreement with experimental ones. This shows that the redistribution of molecules over the different symmetry species of the dyad is well-described by the processes of vibrational swap introduced in the kinetic model.

The difference in the temporal evolution of the signals obtained with H_2 and with He by probing $(2\nu_4 + \nu_3) - 2\nu_4$ transitions can also be well reproduced by taking into account the V−T transfer processes for all excited vibrational states as can be seen in Figure 6 by comparing the calculated signals to the experimental ones.

For V−T transfer processes at room temperature, our results are in fair agreement with the results of refs 10 and 11 for CH_4−He collisions, and they are also in fair agreement with the results of ref 7 for CH_4-H_2 collisions. At 193 K, this is also the case for CH_4−He collisions (refs 10 and 11). Our result at 193 K for CH_4-H_2 collisions cannot be compared with others because it is the first measurement of this rate coefficient.

The results of our simulations for CH_4/H_2 and CH_4/He mixtures using the values given in Table 4 are in good agreement with the experiments both at room temperature and at 193 K, and this is true for all types of probed transitions. Examples of

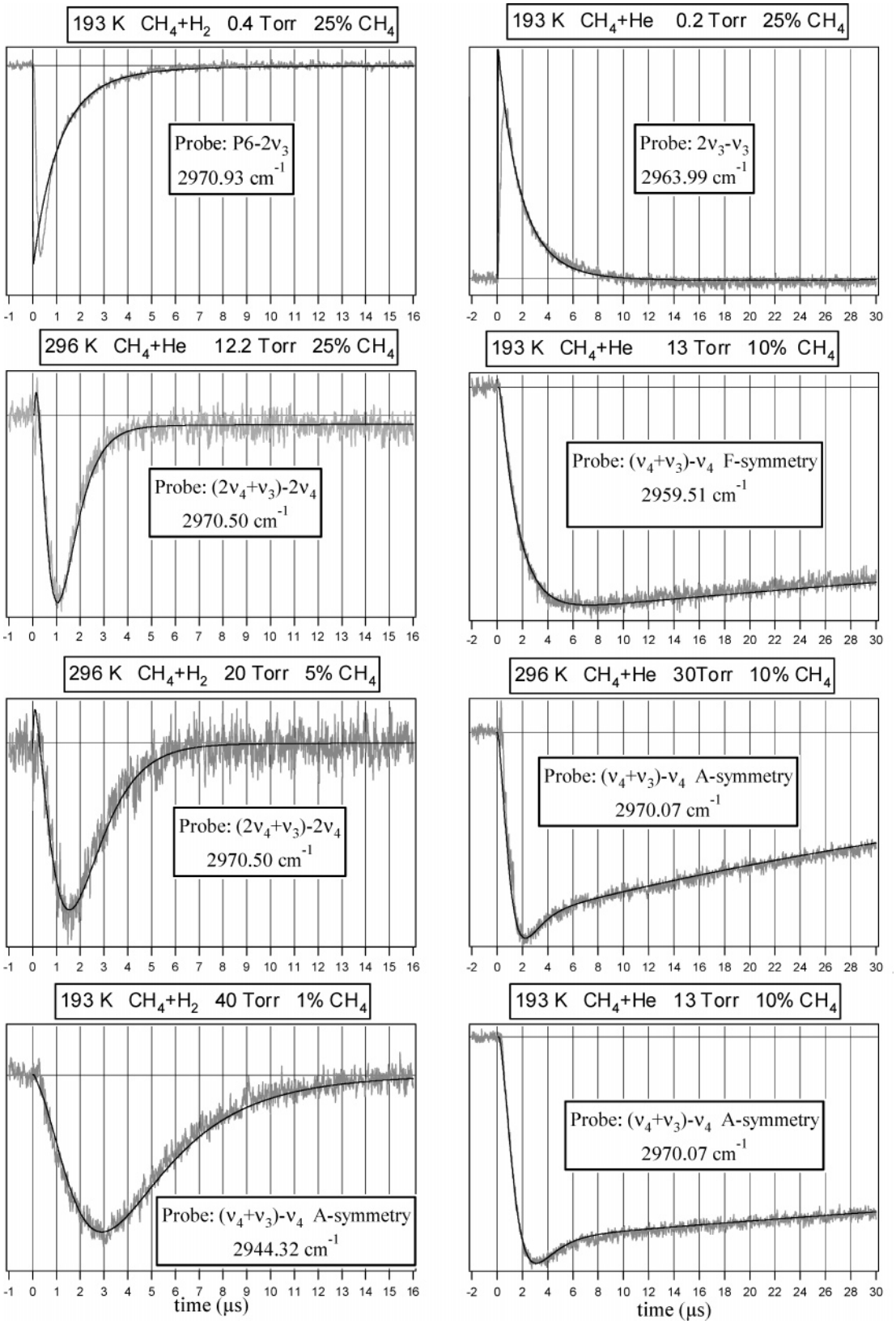

Figure 9. Experimental signals compared to simulated ones for various mixtures at different molar fractions and temperatures. All these signals were obtained by exciting methane into a rovibrational level of A symmetry type.

simulated signals corresponding to representative experimental signals at different temperatures and for various types of probes are shown in Figure 9.

It is difficult to obtain more precise values for the intermode transfer processes. Actually, numerous interactions exist between the various states and substates of a polyad and other intermode transfer processes might be involved in the redistribution of energy over these states, but to refine the present model, it would be necessary to dispose of other probes. A better knowledge of the frequencies of other pentad−tetradecad transitions would be necessary to test the intermode processes introduced in the kinetic model.

V. Conclusion

The good agreement between computed and observed DR signals is encouraging for using this model to predict the time evolution of populations of methane energy levels especially for pressure or mixing ratio values that cannot be realized in our experiments. It is noteworthy that the processes needed to describe the relaxation of methane molecules excited up to energy levels near 6000 cm^{-1} or higher strongly depend on the composition of the gas mixtures and of the temperature. Indeed, the effect of V−T transfer processes relative to V−V transfer processes increases as the molar fraction of methane decreases. At room temperature, the V−T processes become faster than the V−V processes for methane molar fractions lower than 3.2% for CH_4/H_2 mixtures, 0.15% for CH_4/He mixtures, and 0.03% for CH_4/N_2 mixtures. However, the rate coefficients for V−V transfer increase as temperature decreases contrary to the rate coefficients for V−T transfer. At 193 K the V−V processes remain faster than the V−T processes as long as the methane molar fractions are higher than 1.2% for CH_4/H_2 mixtures, 0.04% for CH_4/He mixtures, and 0.01% for CH_4/N_2 mixtures. That means that, at lower temperatures, the V−V processes might play a non-negligible role for the depopulation of the polyads higher than the dyad even at a very small methane molar fraction.

Besides the assigned signals used in this study, numerous DR signals have been observed for probe wavenumbers that are not currently assigned to a transition with well-identified quantum numbers. Among these signals, various ones were found to correspond undoubtedly to pentad−tetradecad transitions between A-symmetry levels. Indeed, these time-resolved DR experiments make it possible to observe and to locate very precisely transitions that could not be observed by traditional spectroscopy. Furthermore, a preliminary identification is possible by comparing the temporal evolution observed for the experimental DR signals corresponding to these unassigned transitions with the temporal evolutions predicted by the kinetic model. In turn, an independent assignment of the detected transitions would be useful to test the intermode processes introduced in the kinetic model.

Acknowledgment. The authors thank Dr. Claude Camy-Peyret for helpful discussions and for his careful reading of the manuscript.

References and Notes

(1) Encrenaz, T.; De Graauw, T.; Schaeidt, S.; Lellouch, E.; Feuchtgruber, H.; Beintema, D. A.; Bezard, B.; Drossart, P.; Griffin, M.; Heras, A.; Kessler, M.; Leech, K.; Morris, P.; Roelfsema, P. R.; Roos-Serote, M.; Salama, A.; Vandenbussche, B.; Valentijn, E. A.; Davis, G. R.; Naylor, D. A. *Astron. Astrophys. (Berl.)* **1996**, *315*, 397.

(2) Lopez-Puertas, M.; Taylor, F. W. In *Non-LTE radiative transfer in the atmosphere*; Taylor, F. W., Ed.; Series on Atmospheric, Oceanic and Planetary Physics; World Scientific Publishing: River Edge, NJ, 2001; Vol. 3.

(3) Klaassen, J. J.; Coy, S. L.; Steinfeld, J. I.; Abel, B. *J. Chem. Phys.* **1994**, *101*, 10533.

(4) Menard-Bourcin, F.; Doyennette, L.; Menard, J.; Boursier, C. *J. Phys. Chem.* **2000**, *104*, 5444.

(5) Menard-Bourcin, F.; Boursier, C., Doyennette, L.; Menard, J. *J. Phys. Chem. A* **2001**, *105*, 11446.

(6) Boursier, C.; Menard, J.; Doyennette, L.; Menard-Bourcin, F. *J. Phys. Chem. A* **2003**, *107*, 5280.

(7) Yardley, J. T.; Fertig, M. N.; Moore, C. B. *J. Chem. Phys.* **1970**, *52*, 1450.

(8) Hess, P.; Moore, C. B. *J. Chem. Phys.* **1976**, *65*, 2339.

(9) Hess, P.; Kung, A. H.; Moore, C. B. *J. Chem. Phys.* **1980**, *72*, 5525.

(10) Perrin, M.-Y.; Jolicard, G. *Chem. Phys. Lett.* **1986**, *127*, 118.

(11) Siddles, R. M.; Wilson, G. H.; Simpson, C. J. S. M. *Chem. Phys.* **1994**, *188*, 99.

(12) The assigned quantum numbers *J*, *C*, and *N* represent the angular momentum, the rovibrational symmetry, and a running number according to increasing energies within the polyads; see Champion, J.-P.; Loëte, M.; Pierre, G. In *Spectroscopy of the Earth's Atmosphere and Interstellar Medium*; Rao, K. N., Weber, A., Eds.; Academic: Columbus, 1992; pp 339−422.

(13) Pine, A. S. *J. Chem. Phys.* **1992**, *97*, 773.

(14) Margolis, J. S. *J. Quant. Spectrosc. Radiat. Transfer* **1993**, *50*, 431.

(15) Varanasi, P.; Chudamani, S. *J. Quant. Spectrosc. Radiat. Transfer* **1989**, *41*, 335.

(16) Varanasi, P. *J. Quant. Spectrosc. Radiat. Transfer* **1971**, *11*, 1711.

(17) Fox, K.; Jennings, D. E.; Stern, E. A.; Hubbard, R. *J. Quant. Spectrosc. Radiat. Transfer* **1988**, *39*, 473.

(18) Zeninari, V.; Parvitte, B.; Courtois, D.; Kapitanov, V. A.; Ponomarev, Yu. N. *Appl. Phys. B* **2001**, *72*, 953.

(19) Darnton, L.; Margolis, J. S. *J. Quant. Spectrosc. Radiat. Transfer* **1973**, *13*, 969.

(20) Varanasi, P.; Sarangi, S.; Pugh, L. *Astrophys. J.* **1973**, *179*, 977.

(21) Robert, O; Champion, J. P. Private communication.

(22) Wenger, Ch.; Champion, J.-P. Spherical Top Data Systems (STDS) software for the simulation of spherical top spectra. *J. Quant. Spectrosc. Radiat. Transfer* **1998**, *59*, 471.